RSC Advances

PAPER

View Article Online
View Journal | View Issue

Cite this: *RSC Adv.*, 2015, **5**, 49420

A ZnO decorated chitosan–graphene oxide nanocomposite shows significantly enhanced antimicrobial activity with ROS generation†

Angshuman Ray Chowdhuri,[a] Satyajit Tripathy,[b] Soumen Chandra,[a] Somenath Roy[b] and Sumanta Kumar Sahu*[a]

The rise in antimicrobial resistance requires the development of new antibacterial agents. Herein, we develop nanocomposites by growing zinc oxide nanoparticles on the surface of chitosan (CS) modified graphene oxide (GO), obtaining GO@CS/ZnO as a novel antibacterial material. The crystal structures, surface functional groups and morphology were analyzed by using X-ray diffraction (XRD) pattern, Fourier transform infrared spectroscopy (FTIR), scanning electron microscopy (SEM) images, respectively. The Minimum Inhibitory Concentration (MIC) and the Minimum Bactericidal Concentration (MBC) of GO@CS/ZnO show more antibacterial potency towards both Gram-negative bacteria *Escherichia coli* (*E. coli*) and Gram-positive bacteria *Staphylococcus aureus* (*S. aureus*). In this study the GO@CS/ZnO expresses its more potency than reported graphene based nanocomposites. Investigation of intercellular reactive oxygen species (ROS) generation, NO generation and catalase activity in *E. coli* and *S. aureus* reveal that GO@CS/ZnO treatment also augments the intracellular bacterial killing by inducing reactive oxygen species production that causes oxidative damage. The minimal inhibition concentrations (MIC) of GO@CS/ZnO against *E. coli* and *S. aureus* are only 2.5 μg mL^{-1} and 5 μg mL^{-1} respectively. Compared with graphene based nanocomposite, which have been widely used as antibacterial agents, our GO@CS/ZnO shows better antibacterial effect. We envision that this study offers novel insights into antimicrobial actions and also demonstrates GO@CS/ZnO is a novel class of topical antibacterial agent in the areas of healthcare and environmental engineering.

Received 26th March 2015
Accepted 27th May 2015

DOI: 10.1039/c5ra05393e

www.rsc.org/advances

1. Introduction

Recently, inorganic nanoparticles have attracted significant interest due to their broad-spectrum and highly effective antibacterial activity.[1–3] The inorganic nanoparticles (NPs) known to have profound antibacterial activity are silver, copper, CuO, TiO_2, $Mg(OH)_2$ and ZnO.[4–9] ZnO nanoparticles are of particular interest because they can be prepared easily and cost effectively. Li *et al.* developed chitosan/ZnO nanocomposites membranes for antibacterial activity.[10] Pascual *et al.* prepared nanocomposites by adding ZnO nanoparticles to bacterial polyester poly(3-hydroxybutyrate-*co*-3-hydroxyvalerate) for antibacterial activity against human pathogenic bacteria.[11] He *et al.* synthesized ZnO/Au hybrid nanostructures for enhanced antibacterial activity.[12]

Till now, ZnO nanoparticle has been widely used as an antibacterial agent. Release of zinc ions and disorder of a bacterial membrane upon contact with ZnO particles were known as antibacterial mechanisms of ZnO NPs.[13] Although various designed ZnO nanoparticles have been utilized against different bacteria, developing ZnO NPs with excellent antibacterial properties is still an attractive challenge. To counter this, we have developed a novel nanocomposite based strategy.

Graphene, a single-atom-thick of carbon atoms closely packed into honeycomb two-dimensional lattice, has attracted wide attention recently. Its sp^2 hybrid carbon framework possesses unique thermal, mechanical, and electrical properties and is being actively explored for potential applications such as nanoelectronics, conductive thin films, supercapacitors, biosensors and nanomedicine. Recently, research attention has been drawn toward the antibacterial activity of graphene oxide and its hybrid materials. Carpio *et al.* evaluated the antimicrobial activity of graphene oxide (GO) silanized with *N*-(trimethoxysilylpropyl) ethylenediamine triacetic acid against Gram-negative, and Gram-positive bacteria.[14] Tang *et al.*

[a]*Department of Applied Chemistry, Indian School of Mines, Dhanbad 826004, Jharkhand, India. E-mail: sahu.s.ac@ismdhanbad.ac.in; sumantchem@gmail.com; Fax: +91 326-2307772; Tel: +91 3262235936*

[b]*Immunology and Microbiology Laboratory, Department of Human Physiology with Community Health, Vidyasagar University, Midnapore-721102, India*

† Electronic supplementary information (ESI) available: EDS spectrum of GO@CS/ZnO nanocomposite, AFM image of GO and GO@CS nanocomposite, schematic presentation of possible mechanism of bactericidal activity of GO@CS/ZnO nano composites. See DOI: 10.1039/c5ra05393e

fabricated GO–Ag nanocomposites with different Ag nanoparticles to GO ratios and investigated their antibacterial activities against both the Gram-negative and the Gram-positive bacteria.[15] The antibacterial activity of GO was attributed to membrane stress induced by sharp edges of graphene nanosheets, which might result in physical damages on cell membranes, leading to the loss of bacterial membrane integrity and the leakage of RNA.[16] Some research has reported that GO sheets show high non-specific binding capability to microbes. However, considering these results, despite the significant efforts, there still exists some challenges to improve the antibacterial activity of graphene nanocomposites.

Chitosan, a copolymer of glucosamine and *N*-acetyl-D glucosamine linked by glycosidic bonds, is the second abundant polymer produced by deacetylation of chitin. Because of its compatibility and biodegradability, chitosan has been used as biomaterial for drug delivery, gene delivery and other biomedical application.[17,18] It is also known that chitosan would show excellent antibacterial activities and have novel synergistic antibacterial effects.[19] Many research groups developed different chitosan based materials for antibacterial effects.[20,21] Some hypotheses indicate that polycationic chitosan could interact with anionic groups on the cell surface thereby causing an increase in membrane permeability and probably disrupting and subsequently facilitating leakage of cellular proteins.[22] The aim of this work is to prepare a chitosan based nanocomposite to improve the antibacterial activity.

In the present study, a new approach is introduce to design a convenient three-component system with synergistic antibacterial effects. Firstly, *exfoliated* graphene oxide nanosheets were prepared by modified Hummer's method, chitosan was layered on GO and ZnO nanoparticles was deposited *in situ* on graphene oxide single layer. Gram-negative *Escherichia coli* and Gram-positive *Staphylococcus aureus* bacteria were used to estimate the antibacterial activity and the human peripheral blood lymphocytes were taken for the cytotoxicity study. This novel nanocomposite demonstrates brilliant stability, long-term antibacterial effect at very low concentrations and mild cytotoxicity. To the best of our knowledge, this three-component GO@CS/ZnO nanocomposite has not been reported despite their great potential applications.

2. Materials and methods

2.1. Materials

Graphite powder was acquired from alfa aesar. Potassium hydroxide, zinc acetate di hydrate, sodium nitrate, sulphuric acid, hydrochloric acid, potassium permanganate, hydrogen peroxide, methanol and ethanol were obtained from Merck India. Chitosan powder (CS) (M_w = 100 000–300 000, deacetylation degree ≥ 90% as determined by free amine groups) was purchased from Sigma Aldrich, 1-[3-(dimethylamino)propyl]-3-ethylcarbodiimide hydrochloride (EDC) and *N*-hydroxysuccinimide (NHS) was procured from Spectrochem, water was Millipore Water. All chemicals are used without further purification. To study the antibacterial activity the following chemicals were used. Luria broth and nutrient broth were procured from Himedia, India. Potassium dihydrogen phosphate (KH_2PO_4), di potassium hydrogen phosphate (K_2HPO_4), and all other chemicals were from Merck Ltd., SRL Pvt., Ltd., Mumbai and were of the highest grade available.

2.2. Preparation of graphene oxide (GO)

Water soluble Graphene Oxide (GO) nanosheets were prepared by modified Hummer's method.[23] Briefly, 1 g of graphite powder and 1 g of sodium nitrate were placed into a 250 mL round bottom flask cooled at 0 °C. Then, concentrated H_2SO_4, 50 mL, was added to the mixture. The mixture was stirred for 30 min at 5 °C for homogenization. Subsequently, 7 g of $KMnO_4$ was added to the reaction system gradually over 1 hour. The temperature of the mixture was retained below 20 °C. The temperature of the reaction system was then elevated to 35 °C and stirred for 2 hours. Afterwards, 90 mL of ultrapure water was slowly added into the paste like product, and the temperature of the reaction system jumped to 95 °C immediately. Finally, 3 mL of 30% H_2O_2, and 55 mL of ultrapure water were poured into the reaction system resulting in the formation of yellowish brown suspension. The solid product, graphite oxide, was separated from the reaction mixture by filtration. The yellowish brown solid powders were washed for three times with diluted HCl (3%), and then dispersed in ultrapure H_2O. Exfoliation of graphite oxide was approached by sonicating the graphite oxide in water at room temperature for 1 h generating uniform graphene oxide dispersions. Finally GO nanosheets were filtered and dried at 35 °C under vacuum oven.

2.3. Preparation of graphene oxide and zinc oxide nanocomposite (GO/ZnO)

To prepare a graphene oxide and zinc oxide nanocomposite (GO/ZnO), 0.10 g of GO suspension in 10 mL water was prepared (solution 1). The mixture was sonicated in ultra-sonication and kept stirring for 10 min. Then 0.7 g of zinc acetate dihydrate was dissolved in 30 mL methanol (solution 2). Solution 1 was added slowly to solution 2, sonicated and stirred for 15 min. Then the mixture was transferred to 100 mL round bottom flask. Potassium hydroxide solution was prepared by adding 0.3 g of KOH in 10 mL of methanol and added slowly to the above solution, the reaction was continued to 8 h at 60 °C. The precipitates was collected by centrifugation at 15 000 rpm for 10 min and washed three times by methanol–water mixture to remove impurities.

2.4. Preparation of graphene oxide chitosan nanocomposite (GO@CS)

For preparation of the GO@CS nanocomposites, 0.10 g of chitosan (CS) was dissolved in 100 mL 1% acetic acid solution and stirred for 1 h. 0.15 g of as synthesized GO was dispersed in 20 mL water and 0.15 g EDC and 0.1 g of NHS was added to the GO suspension, and stirred for 3 h. Then GO suspension was added to chitosan solution very slowly and stirred for 12 h. Finally Product was collected by centrifugation at 15 000 rpm for 10 min and dried at 35 °C under vacuum oven.

2.5. Preparation of graphene oxide, chitosan and zinc oxide nanocomposite (GO@CS/ZnO)

For preparation of GO@CS/ZnO nanocomposite, firstly as synthesized 0.1 g GO@CS was dispersed in 10 mL water. The mixture was sonicated in ultra-sonication and kept stirring for 10 min (solution 1). Then 0.7 g of zinc acetate dihydrate was dissolved in 30 mL methanol (solution 2). Solution 1 was added slowly to solution 2, sonicated and stirred for 15 min. Then the mixture was transferred to 100 mL round bottom flask. Potassium hydroxide solution was prepared by adding 0.3 g of KOH in 10 mL of methanol and added slowly to the above solution, the reaction was continued to 8 h at 60 °C. The precipitates was collected by centrifugation at 15 000 rpm for 10 min and washed three times by methanol–water mixture to remove impurities and dried at 35 °C under vacuum oven.

2.6. Preparation of zinc oxide nanoparticles (ZnO NP) and zinc oxide chitosan nanocomposite (ZnO@CS)

To prepare the zinc oxide nanoparticles, 0.7 g of zinc acetate dihydrate was dissolved in 30 mL methanol. Potassium hydroxide solution was prepared by adding 0.3 g of KOH in 10 mL of methanol and added slowly to the above solution, the reaction was continued to 8 h at 60 °C. The white precipitates was collected by centrifugation at 15 000 rpm for 10 min and washed three times by methanol–water mixture to remove impurities. The products was dried in a vacuum oven at 50 °C.

For the preparation of zinc oxide chitosan nanocomposite (ZnO@CS), 0.01 g of chitosan was dissolved in 30 mL 0.05% acetic acid solution and 0.2 g of above synthesized ZnO NP was dispersed in the prepared chitosan solution. The reaction was continued to 6 h. The precipitates was collected by centrifugation at 15 000 rpm for 10 min and washed three times by methanol–water mixture to remove impurities. The products was dried in a vacuum oven at 50 °C.

2.7. Instrumentation

Attachment of surface functional groups was investigated by FTIR spectroscopy (Thermo Nicolet Nexus FTIR (model 870)). The phase formation and crystallographic state of grapheme oxide, chitosan coated graphene oxide and ZnO deposited nanocomposite were determined by XRD with an Expert Pro (Phillips) X-ray diffractometer using Cu Kα. To investigate the surface morphology, FESEM analysis was performed by Supra 55 with Air Lock chamber for scientific research. Energy Dispersive Microanalysis was carried out to for elemental investigation. Atomic force microscopy (AFM) was done by Bruker dimension icon nanoscope (Germany). For this, the sample was dropouts on a clean glass plate and vacuum dried in room temperature. The fluorescence intensity of each sample was analyzed under fluorescent microscope (Hitachi 7400) for detection of fluorescence intensity (excitation and emission wavelengths were 495 nm and 529 nm respectively) in bacterial cells.

2.8. *In vitro* cytotoxicity of GO@CS/ZnO by MTT assay

The human peripheral blood lymphocytes were isolated and cultured in Dulbecco Modified Eagle's medium (DMEM) and Minimal Essential Medium (MEM) supplemented with 10% fetal calf serum, 100 units per mL penicillin and 100 μg mL^{-1} streptomycin, 4 mM L-glutamine under 5% CO_2 and 95% humidified atmosphere at 37 °C. Cells were seeded into 96 wells of tissue culture plates with media and were incubated for 24 h. GO@CS/ZnO composites were added to the cells at different concentrations were incubated for 24 h at 37 °C in a humidified incubator maintained with 5% CO_2. The cell viability was estimated by 3-(4,5-dimethylthiazol)-2-diphenyltertrazolium bromide (MTT).[24]

2.9. Bacterial suspension preparation

The bacterial strain of Gram-positive bacteria (*Staphylococcus aureus* ATCC 25923) and Gram-negative bacteria (*Escherichia coli* ATCC 25922) were grown at 37 °C overnight in nutrient agar broth. The bacterial culture was centrifuged at 5000 rpm for 15 minutes. The pallets were resuspended and washed with sterile phosphate buffer saline (PBS). The bacterial suspension was adjusted by serial dilution in PBS to final concentration of approximately 5×10^6 in 100 μL by using a UV-spectrophotometer (Schimadzu, USA) at an absorbance of 620 nm. From this suspension, the bacteria were cultured in 1 mL nutrient agar broth and the culturable bacterial count was adjusted to approximately 1.0×10^9 colony-forming units (CFU) mL^{-1}.

2.10. Determination of minimum inhibitory concentration (MIC)

The minimum inhibitory concentration (MIC) of the GO, GO@CS, GO/ZnO, ZnO@CS, GO@CS/ZnO and ZnO were determined against Gram-positive bacteria (*S. aureus*) and Gram-negative bacteria (*E. coli*) by a slight modification of the described method of the National Committee for Clinical Laboratory Standards (NCCLS).[25] The MIC value of the nanocomposite was that concentration of the nanocomposite where no visible growth appeared in the broth tube.

2.11. Determination of minimum bactericidal concentration (MBC)

The minimum bactericidal concentration (MBC) of the GO, GO@CS, GO/ZnO, ZnO@CS, GO@CS/ZnO and ZnO were evaluated against *S. aureus* and *E. coli* by slight modification of the method described by Ericsson and Sherris in 1971.[26] After the MIC test, bacteria from each test tube were charged on an MHA plate and checked overnight at 37 °C. The MBC value of the nanocomposite was that concentration, where no visible growth appeared on the agar plate.

2.12. Determination of the growth curves of bacterial cells

To examine the growth curves of bacterial cells exposed to GO@CS/ZnO, Mueller-Hinton broth with MIC concentrations (*E. coli*: 2.5 μg mL^{-1}; *S. aureus*: 5 μg mL^{-1}) was used, and the

bacterial cell concentration was adjusted initially at 10^6 CFU mL^{-1}. Each culture was incubated in a shaking incubator at 37 °C for 24 h. Growth curve has been presented by colony forming units at different time interval.

2.13. Determination of intracellular ROS

Measurements of intracellular ROS levels in treated bacteria at MIC concentration were made using 2′,7′-dichlorodihydrofluorescein diacetate ($DCFH_2$-DA). Samples were incubated in the presence of 10 mM $DCFH_2$-DA in phosphate buffered saline (PBS) at 37 °C for 30 min then washed two times with PBS and centrifuged at 1200 rpm to remove the extracellular $DCFH_2$-DA. The trapped fluorescent dye (DCF) inside the cells was used to evaluate and detect intracellular ROS. The fluorescence values at different conditions were monitored by excitation at 498 nm and emission 530 nm.[27]

2.14. Determination of NO generation

NO generation was determined according to the method of Sanai *et al.*[28] In brief, 100 μL of Griess reagent (containing 1 part of 1% sulfanilamide in 5% phosphoric acid, and 1 part of 0.1% of N-C-1napthyl ethylene diamine dihydrochloride) was added to 100 μL of sample, incubated at room temperature for 10 minutes, readings were taken in a UV spectrophotometer at 550 nm and compared to a sodium nitrite standard curve (values ranging between 0.5 and 25 μM). The level of NO was expressed as μM mg^{-1} protein.

2.15. Determination of CAT activity

Catalase activity was measured by the method of Luck.[29] The final reaction volume of 3 mL contained 0.05 M Tris-buffer, 5 mM EDTA (pH 7.0), and 10 mM H_2O_2 (in 0.1 M potassium phosphate buffer, pH 7.0). About 50 μL aliquot of the lysates was added to the above mixture. The rate of change of absorbance per min at 240 nm was recorded. Catalase activity was calculated by using the molar extinction coefficient of 43.6 L M^{-1} cm^{-1} for H_2O_2. The level of catalase was expressed in terms of mmol H_2O_2 consumed/min mg protein.

2.16. Morphology investigation of bacteria after contact to the GO@CS/ZnO nanocomposites

To investigate the detail change of morphology of bacteria surface membrane after treatment with the GO@CS/ZnO nanocomposites, *E. coli* and *S. aureus* were cultured in a LB culture medium containing different concentration of GO@CS/ZnO for 24 h. Upon centrifugation at 5000 rpm for 10 min, the bacteria were collected and washed with phosphate-buffered saline twice and then suspended in Millipore water. The suspension was filtered through a polycarbonate filter (Whatman nucleopore 0.2 μm) and was fixed in a glutaraldehyde solution at 4 °C for 2 h. Upon repeated rinses with double-distilled water, the specimen was dehydrated successively with graded ethanol solutions: 50% for 30 min, 75%, 85%, and 95% each for 10 min, and 100% for 10 min twice. Then the specimen was subjected to vacuum drying to remove ethanol completely. Finally, it was stacked onto a carbon tape and examined under a field emission scanning electron microscope.

2.17. Protein estimation

Protein was determined according to Lowry *et al.* using bovine serum albumins as standard.[30]

2.18. Data analysis

The data were expressed as mean ± standard error, $n = 3$. The statistical analysis were done by a model I ANOVA test (using a statistical package, Origin 6.1, Northampton, MA 01060, USA) with multiple comparison t tests, $P < 0.05$ as a limit of significance.

3. Results and discussion

3.1. FTIR study

The presence of GO, CS and ZnO individually in GO@CS@ZnO nanocomposite was confirmed using FTIR spectroscopy. The distinctive features of GO in the FTIR spectra corresponding to the C=O carbonyl stretching at 1720 cm^{-1}, the C–OH stretching at 1224 cm^{-1}, and the C–O stretching at 1050 cm^{-1}.[31] The spectra also show a C=C peak at 1620 cm^{-1} corresponding to the remaining sp^2 character,[31] a very broad intense peak at 3430 cm^{-1} for O–H stretching frequencies. Peaks at 1095 cm^{-1} and 1393 cm^{-1} are also the characteristics peaks for C–O–C and C–OH stretching vibration frequency of GO.[32] Fig. 1 shows the characteristics peaks of CS at 3440, 2858, 1647, 1566, 1161, 1057 cm^{-1}.[33] It was observed that, CS, GO@CS and GO@CS/ZnO exhibit peaks in the region of 2858 cm^{-1}, which are assigned to the symmetric and asymmetric modes of CH_2 group vibrations. It is confirmed that the CS is successfully formed a layer on the surface of GO. The sharp peak at 458 cm^{-1} for Zn–O stretching frequency confirms that ZnO is effectively bind both GO and GO@CS.

3.2. XRD study

The X-ray diffraction pattern of graphene oxide synthesized by modified Hummer's Method is shown in Fig. 2(a). A sharp peak at $2\theta = 11.3°$ is corresponding to the (001) diffraction peak of

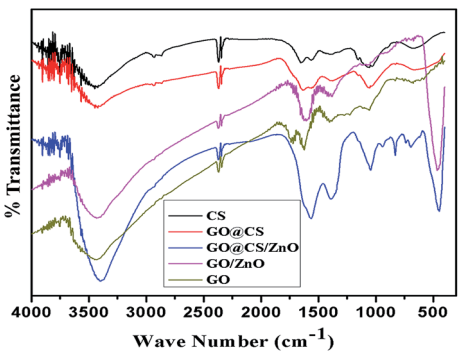

Fig. 1 FTIR spectra of GO, CS, GO@CS, GO/ZnO and GO@CS/ZnO nanocomposite.

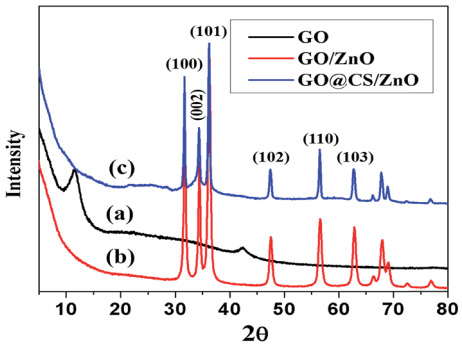

Fig. 2 Powder X-ray diffraction patterns of (a) GO; (b) GO/ZnO; (c) GO@CS/ZnO.

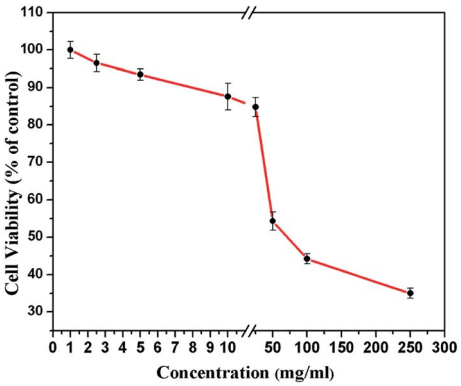

Fig. 4 Graphical presentation represents the percentage (%) of viable lymphocytes after treatment with GO@CS/ZnO at different concentration by MTT assay.

disordered GO.[34] The presence of ZnO nanoparticles in the GO layer was confirmed by the XRD analysis shown in Fig. 2(b). The characteristics peaks observed at $2\theta = 31.7°$, 34.36°, 36.14°, 47.58°, 56.52°, 62.76°, 67.96°, 69.10°, 72.31° are corresponding to the (1 0 0), (0 0 2), (1 0 1), (1 0 2), (1 1 0), (1 0 3), (1 1 2), (2 0 1), (0 0 4) crystalline planes, respectively, of ZnO nanoparticles [JCPDS card no: 80-0074]. Suddenly, the peak at $2\theta = 11°$ (due to the stacking of the GO layers) disappeared when the ZnO nanoparticles were formed on GO layer.[35] This phenomenon is due to the anchoring of ZnO nanoparticles on the surface of the GO sheets prevents the stacking of the GO layers.[35] XRD Pattern of GO@Cs/ZnO nanocomposite exhibited Peak at $2\theta = 14.5°$, 59° and a broad peak above 20° confirms that the existence of amorphous state of the chitosan,[33,36,37] shown in Fig. 2(c).

3.3. Surface morphology study

The surface morphology of GO@CS/ZnO tricomponent system was explored by Field Emission Scanning Electron Microscopy. Fig. 3(a) represents that the genuine size of the synthesized GO sheets with wrinkles. The thickness of the sheets are less than 5 nm, which are able to offer fantastic antibacterial capability due to exfoliation of single GO sheets in water.[38] FESEM image of GO@CS demonstrates that appearance of CS into π–π stacking of GO nanosheets not disturbed the exfoliation of GO. The GO sheets are uniformly covered by CS as shown in Fig. 3(b).[33] Fig. 3(c) shows the morphology of morphology of the synthesized ZnO nanoparticles. Fig. 3(d) shows that the direct evidence of deposition of ZnO NPs onto GO nanosheets with a range of 30 nm. The wrinkles of the GO nanosheets (indicated by arrow) are the witness of the thin nanosheets are not disturbed during the formation of ZnO nanoparticles on the GO layers. *In situ* formation of ZnO NPs are well decorated on the GO@CS layers, shows the superior antibacterial activity shown in the Fig. 3(e) and (f). The density of ZnO NPs on the GO@CS/ZnO nanocomposite is very high, indicates the strong interaction of ZnO with the layer of GO@CS.

The energy dispersive spectroscopy (EDS) confirms the presence of Zn, O, C, and N in the GO@CS/ZnO nanocomposites: data are shown in Fig. S1.† Throughout the scanning range of binding energies, no obvious peak belonging to impurity is detected. The result indicates that the product is composed of high purity nanocomposites.

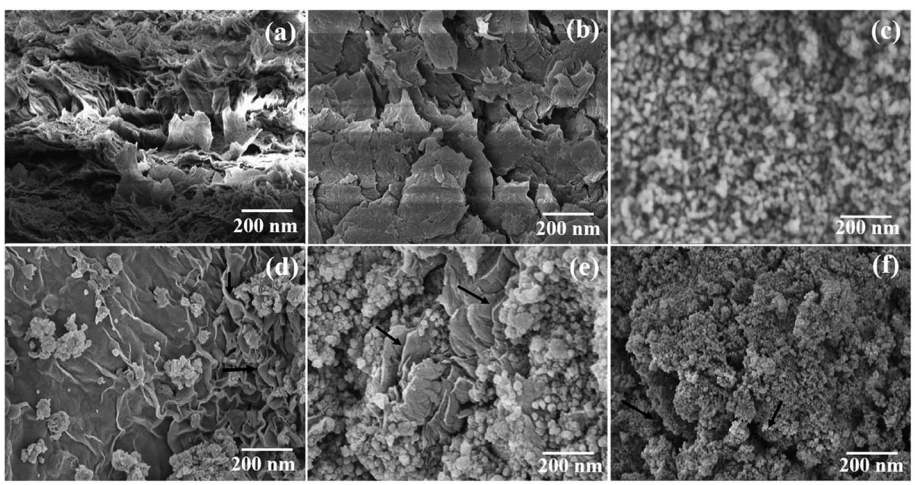

Fig. 3 FESEM images of (a) GO; (b) GO@CS; (c) ZnO; (d) GO/ZnO; (e and f) GO@CS/ZnO.

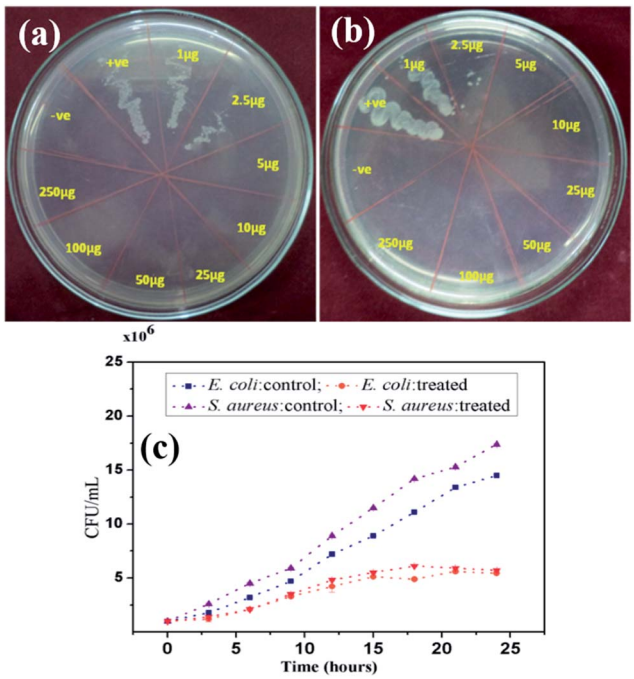

Fig. 5 MBC study of GO@CS/ZnO at MIC concentration against (a) *S. aureus* and (b) *E. coli* (c) comparison of growth pattern of *S. aureus* (at 5 μg mL^{-1}) and *E. coli* (at 2.5 μg mL^{-1}).

Table 1 Minimum Inhibitory Concentration (MIC) of different synthesized composites against *S. aureus* and *E. coli*

	Minimum Inhibitory Concentration	
Particles	*Staphylococcus aureus*	*Escherichia coli*
1. GO	250 μg mL^{-1}	100 μg mL^{-1}
2. GO@CS	25 μg mL^{-1}	25 μg mL^{-1}
3. GO/ZnO	50 μg mL^{-1}	50 μg mL^{-1}
4. GO@CS/ZnO	5 μg mL^{-1}	2.5 μg mL^{-1}
5. ZnO	100 μg mL^{-1}	100 μg mL^{-1}
6. ZnO@CS	100 μg mL^{-1}	50 μg mL^{-1}

3.4. Cytotoxicity assay of the GO@CS/ZnO composites

To test the cytotoxicity of the composites to other species, peripheral blood mononuclear cells (PBMC) were selected. The viability of PBMC cells was assayed after exposure to GO@CS/ZnO composites by MTT assay (Fig. 4). In the method, MTT is reduced to a purple formazan by NADH. The cell viability loss induced by the composites is dose-related. GO@CS/ZnO exposure at 25 μg mL^{-1}, showed >80% cells have mitochondrial dehydrogenase activities which represents the viability, indicating the low toxicity of GO@CS/ZnO to PBMC. However, over 50 μg mL^{-1}, NAD(P)H-dependent cellular oxidoreductase enzymes of more than 50% cells are not capable of reducing the tetrazolium dye MTT 3-(4,5-dimethylthiazol-2-yl)-2,5-diphenyltetrazolium bromide to its insoluble formazan, which has a purple color, it may be due to the higher amount containing the ZnO particles, so, when the concentration of the composites increases to 250 μg mL^{-1} the viability decreased obviously.

3.5. Bactericidal efficiency of the GO@CS/ZnO composites

To evaluate the efficacy of anti-bacterial activity of synthesized GO@CS/ZnO composites we compared by minimum inhibitory concentration study and MBC study of only, GO, GO@CS, GO/ZnO, GO@CS/ZnO, ZnO@CS and ZnO against Gram-positive *S. aureus* and Gram-negative *E. coli*. We found that the GO@CS/ZnO is able to inhibit the bacterial growth at minimum concentration, 5 and 2.5 μg mL^{-1} against *S. aureus* and *E. coli* respectively, whereas only GO, GO@CS, GO/ZnO, ZnO@CS and ZnO showed minimum inhibitory activity (shown in Table 1) and MBC activity at more higher concentration. Fig. 5 represent the MBC results of only GO@CS/ZnO against *S. aureus* and *E. coli*.

After evaluating the MIC concentration of GO@CS/ZnO against bacteria we compared the growth pattern between non treated bacterial cells and GO@CS/ZnO charged bacterial cells. The results revealed that the bacterial growths of cells treated with GO@CS/ZnO nanocomposites were inhibited as shown in Fig. 5(C).

In addition to its additional antibacterial activity, it is well known that chitosan has some important advantages such as biocompatibility, non-toxicity and biodegradability. Chitosan is very easily stacked onto to the graphene oxide layer. Chitosan is a cationic polysaccharide derived from chitin, having a positive surface charges. So, it is attracted towards the negatively charged cell membrane of the both gram positive and gram negative bacteria and enhanced the attachment of GO@CS/ZnO nanocomposite and bacteria.

Oxidative stress is a highly recognized mechanism for the antimicrobial activity of various NPs. A systematic study was performed to evaluate whether GO is able to induce oxidative stress in bacterial cell. Due to the structural and physiochemical properties of carbon nanomaterials such as fullerene,[39] which induce oxidative stress as a key antibacterial mechanism. In another side, it is also reported that ZnO induce ROS to kill the bacteria.[40] ZnO NPs was assumed to be responsible for the high antibacterial performance of ZnO NPs by initiating disorganization of the cell membrane and also ZnO damaged the membrane by releasing the zinc ion and producing the reactive oxygen species that is ROS dependent oxidative stress. But in case of GO, ROS independent oxidative stress is reported. Glutathione (GSH) oxidation is the possibility of ROS-independent oxidative stress mediated by GO. GSH is a tripeptide with thiol groups. It is an antioxidant in bacteria can prevent damages to cellular components caused by oxidative stress. In this study, authors supposed with the mechanism and our current MIC results showed that ZnO have better activity than GO in peptidoglycan rich bacteria and it may be due to the based on superoxide anion production. It suggest due to the trace amount of ROS production by ZnO, but in case of GO, it plays a minor role in the antibacterial activity. Here, our study revealed that ZnO based graphene oxide materials mediate a ROS production and a trace amount of ROS may be produced; this plays a role in the antibacterial activity of graphene-based materials. To investigate ROS production as one of the key factors for cell death, we measured ROS levels using $DCFH_2$ DA staining as shown in Fig. 6. The results showed that the ROS

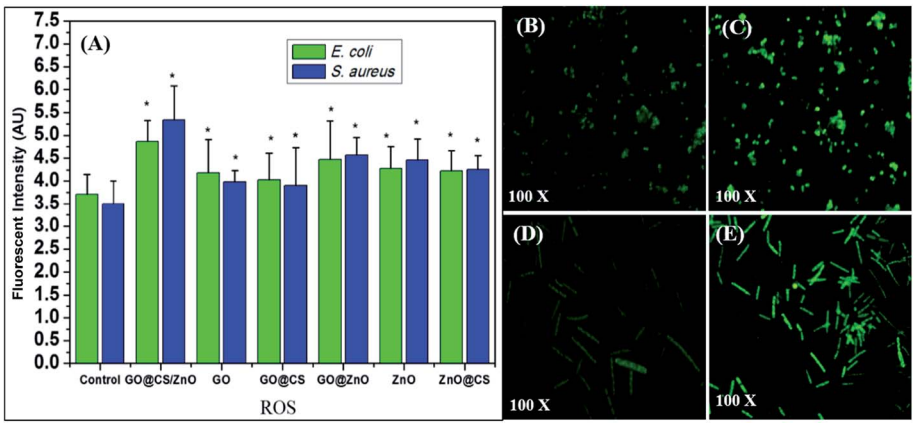

Fig. 6 Graphical presentation (A) of mean fluorescent intensity of bacterial cells of control, and treated with GO@CS/ZnO, GO, GO@CS, GO/ZnO, ZnO and ZnO@CS at MIC concentration. Values are expressed as mean ± SEM, $n = 4$. *Significant difference ($P < 0.05$) compared to control. Intracellular ROS generation. Fluorescent microscopic image (100× magnifications) of $DCFH_2DA$ stained bacteria (B) *S. aureus* control; (C) *S. aureus* after treatment with GO@CS/ZnO at MIC concentration; (D) *E. coli* control; (E) *E. coli* after treatment with GO@CS/ZnO at MIC concentration.

significantly increased in both GO@CS/ZnO charged (at MIC concentration) *S. aureus* and *E. coli* compared to control bacterial cells. To be confirm about the oxidative stress mediated bacterial death, we evaluated the NO level and catalase activity in GO@CS/ZnO charged bacteria after treatment as shown in Fig. 7. The NO generation was increased significantly ($P < 0.05$) in *S. aureus* and *E. coli* but catalase activity decreased in both cases. The ROS generation (Fig. 6), NO generation (Fig. 7(A)) and catalase activity (Fig. 7(B)) after treatment with GO@CS/ZnO, GO, GO@CS, GO/ZnO, Zn@CS and ZnO, indicates that the both *S. aureus* and *E. coli* are more susceptible to GO@CS/ZnO rather than other synthesized nanocomposites.

This study suggests that GO@CS/ZnO causes ROS generation in the bacteria. It is proposed that active superoxide ions are generated on the surface of the oxide, which can react with the peptide linkages in the cell wall of bacteria and thus disrupt.[41,42] Here, the bactericidal action of GO@CS/ZnO may results from attack of these superoxide ions on carbonyl group in the peptide linkages, leading to degradation of the proteins. As the surface area of the particles increases, it leads to an increase of the O_2^- concentration in solution causes oxidative imbalance in bacteria and consequences in a more efficient damage of the cell wall of the bacteria.

3.6. Bacterial morphology

The very low concentration of three component GO@CS/ZnO nanocomposite successfully inhibited the growth of *E. coli* and *S. aureus*. The change of morphology and cell rupture of the bacterium is investigated by FESEM as shown in Fig. 8. The morphology of untreated *E. coli* and *S. aureus*. Untreated *E. coli* (control) and *S. aureus* (control) were rod-shaped and round-shaped respectively, with smooth and unbroken cell walls.[15] However, the *E. coli* cells treated with 1 μg mL^{-1}, 2.5 μg mL^{-1}, 10 μg mL^{-1} of GO@CS/ZnO nanocomposite [Fig. 8(b)–(d)] and *S. aureus* cells treated with 2.5 μg mL^{-1}, 10 μg mL^{-1}, 20 μg mL^{-1} of GO@CS/ZnO nanocomposite [Fig. 8(f)–(h)] exhibited significant morphological deviations, and the structure of the cell walls damaged significantly [indicated by arrows]. This images proved that GO@CS/ZnO nanocomposite leaked out the *E. coli* and *S. aureus* cells. Primarily, the GO sheets adsorb and gather the bacteria onto the sheets, which may enhance the contact between

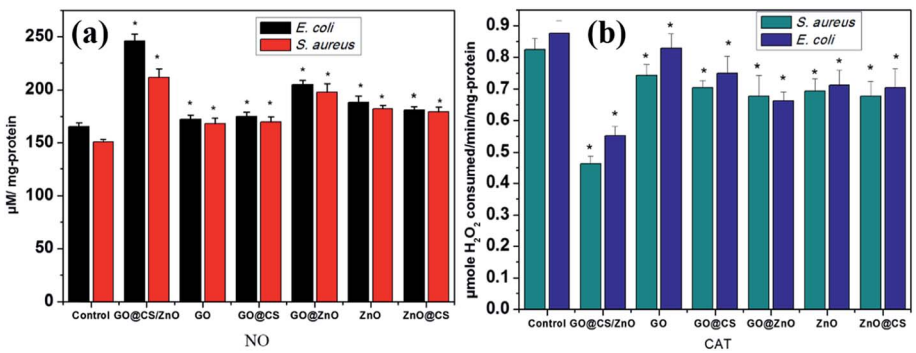

Fig. 7 Graphical presentation represents the (a) NO generation in bacterial cells (b) catalase activity after treatment with GO@CS/ZnO, GO, GO@CS, GO/ZnO, ZnO and ZnO@CS at MIC concentration against *S. aureus* and *E. coli*. Values are expressed as mean ± SEM, $n = 4$. *Significant difference ($P < 0.05$) compared to control.

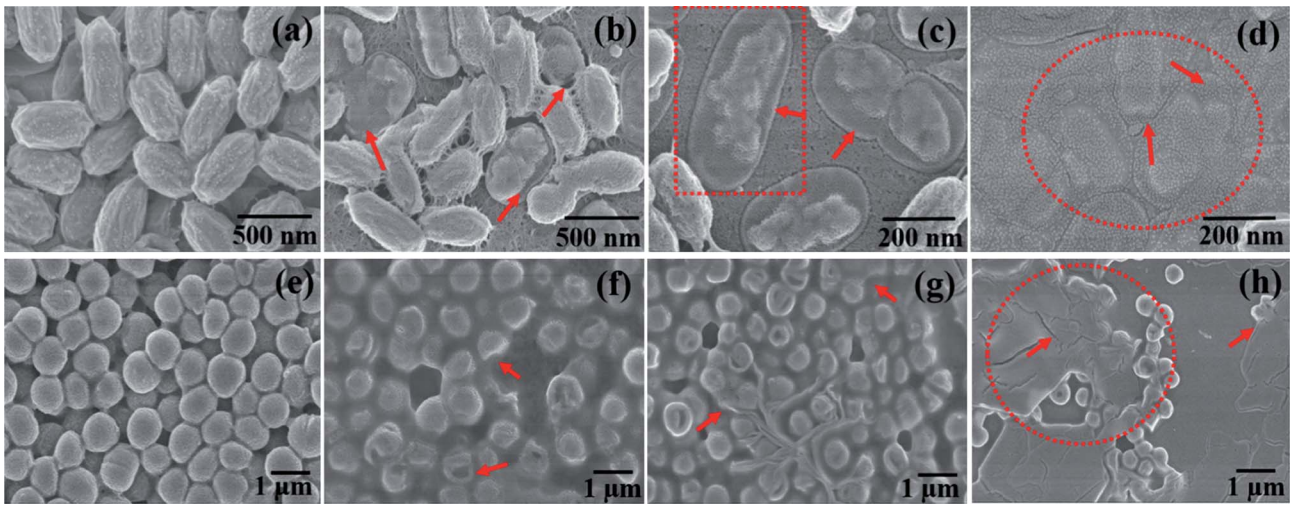

Fig. 8 FESEM images showing the morphology of (a) *E. coli* (control); (e) *S. aureus* (control) (b) *E. coli*, treated with 1 μg mL^{-1}, (c) 2.5 μg mL^{-1} (d) 10 μg mL^{-1} at 12 h; (f) *S. aureus* treated with 2.5 μg mL^{-1}, (g) 10 μg mL^{-1} (h) 20 μg mL^{-1} at 12 h.

bacteria and ZnO nanoparticles on GO sheets. The exposure of ZnO nanoparticles in bacterial suspension would ensure continuous release of zinc ions or produce ROS and ruptured them, thereby leading to protein denaturation and cell death.

4. Conclusion

In summary, we have developed a new approach toward the synthesis of highly efficient GO@CS/ZnO nanocomposite at mild temperature. The GO@CS/ZnO served as the more potential antibacterial agent against both *E. coli* and *S. aureus*. The intimate contact of the bacterial cells and ZnO NPs on the GO@CS enhanced the permeability of the bacterial membrane and generate active superoxide ions (O_2^-), which can react with the peptide linkages in the cell wall of bacteria and thus disrupt. In the future, the GO@CS/ZnO nanocomposites, containing formulations with high antibacterial ability and low toxicity may be utilized promisingly as disinfection agents to electively inhibit bacterial growth.

Author contributions

The manuscript was written through contributions of all authors. All authors have given approval to the final version of the manuscript.

Acknowledgements

The authors would like to acknowledge their institute, Indian School of Mines, Dhanbad for fundamental research support.

References

1 H. Tang, A. Lu, L. Li, W. Zhou, Z. Xie and L. Zhang, *Chem. Eng. J.*, 2013, **234**, 124–131.
2 J. J. Lin, W. C. Lin, S. D. Li, C. Y. Lin and H. Hsu, *ACS Appl. Mater. Interfaces*, 2013, **5**, 433–443.
3 Y. Li, W. Zhang, J. Niu and Y. Chen, *ACS Nano*, 2012, **6**(6), 5164–5173.
4 A. Ray Chowdhuri, S. Tripathy, C. Haldar, S. Chandra, B. Das, S. Roy and S. K. Sahu, *RSC Adv.*, 2015, **5**, 21515–21524.
5 M. Veerapandian, S. Sadhasivam, J. Choi and K. Yun, *Chem. Eng. J.*, 2012, **209**, 558–567.
6 A. Y. Booshehri, R. Wang and R. Xu, *Chem. Eng. J.*, 2015, **262**, 999–1008.
7 R. A. Arain, Z. Khatri, M. H. Memon and I. S. Kim, *Carbohydr. Polym.*, 2013, **96**, 326–331.
8 X. Pan, Y. Wang, Z. Chen, D. Pan, Y. Cheng, Z. Liu, Z. Lin and X. Guan, *ACS Appl. Mater. Interfaces*, 2013, **5**, 1137–1142.
9 S. Selvam and M. Sundrarajan, *Carbohydr. Polym.*, 2012, **87**, 1419–1424.
10 L. H. Li, J. C. Deng, H. R. Deng, Z. L. Liu and L. Xin, *Carbohydr. Res.*, 2010, **345**, 994–998.
11 A. M. Díez-Pascual and A. L. Díez-Vicente, *ACS Appl. Mater. Interfaces*, 2014, **6**, 9822–9834.
12 W. He, H. K. Kim, W. G. Wamer, D. Melka, J. H. Callahan and J. J. Yin, *J. Am. Chem. Soc.*, 2014, **136**, 750–757.
13 Y. W. Wang, A. Cao, Y. Jiang, X. Zhang, J. H. Liu, Y. Liu and H. Wang, *ACS Appl. Mater. Interfaces*, 2014, **6**, 2791–2798.
14 I. E. M. Carpio, J. D. Mangadlao, H. N. Nguyen, R. C. Advincula and D. F. Rodrigues, *Carbon*, 2014, **77**, 289–301.
15 J. Tang, Q. Chen, L. Xu, S. Zhang, L. Feng, L. Cheng, H. Xu, Z. Liu and R. Peng, *ACS Appl. Mater. Interfaces*, 2013, **5**, 3867–3874.
16 O. Akhavan and E. Ghaderi, *ACS Nano*, 2010, **4**(10), 5731–5736.
17 S. K. Sahu, S. Maiti, A. Pramanik, S. K. Ghosh and P. Pramanik, *Carbohydr. Polym.*, 2012, **87**, 2593–2604.
18 S. Tang, Z. Huang, H. Zhang, Y. Wang, Q. Hu and H. Jiang, *Carbohydr. Polym.*, 2014, **101**, 104–112.
19 S. Chen, Y. Guo, S. Chen, H. Yu, Z. Ge, X. Zhang, P. Zhangd and J. Tang, *J. Mater. Chem.*, 2012, **22**, 9092–9099.

20 P. Petkova, A. Francesko, M. M. Fernandes, E. Mendoza, I. Perelshtein, A. Gedanken and T. Tzanov, *ACS Appl. Mater. Interfaces*, 2014, **6**, 1164–1172.
21 S. Mallick, S. Sharma, M. Banerjee, S. S. Ghosh, A. Chattopadhyay and A. Paul, *ACS Appl. Mater. Interfaces*, 2012, **4**, 1313–1323.
22 A. M. Abdelgawad, S. M. Hudson and O. J. Rojas, *Carbohydr. Polym.*, 2014, **100**, 166–178.
23 C. Li, X. Wang, F. Chen, C. Zhang, X. Zhi, K. Wang and D. Cui, *Biomaterials*, 2013, **34**, 3882–3890.
24 S. Tripathy, S. Chattopadhyay, S. P. Chakraborty, S. K. Dash, A. Ray Chowdhuri, S. Das, S. K. Sahu, S. Majumdar and S. Roy, *Int. J. Biol. Macromol.*, 2015, **74**, 585–600.
25 NCCLS 2000Approved Standard M7-A55th edn, vol 17, no. 2 (Wayne, PA: NCCLS).
26 H. M. Ericsson and J. C. Sherris, *Acta Pathol. Microbiol. Scand., Sect. B: Microbiol. Immunol.*, 1971, **217**, 1–10.
27 S. Tripathy, S. KarMahapatra, S. Chattopadhyay, S. Das, S. K. Dash, S. Majumder, P. Pramanik and S. Roy, *Acta Trop.*, 2013, **128**, 494–503.
28 S. Sanai, M. Tomisato, N. Shinsuka, Y. Mayoko, H. Mayoko and N. Akio, *Infect. Immun.*, 1998, **66**, 1017–1028.
29 H. Luck Catalase, in *Methods of Enzymatic Analysis*, ed. H. W. Bergmeyer, Academic Press, New York, 1963, section 3, pp. 885–894.
30 O. H. Lowry, N. J. Rosenbrough, A. L. Farr and R. J. Randall, *J. Biol. Chem.*, 1951, **193**, 255–275.
31 L. Liu, C. Li, C. Bao, Q. Jia, P. Xiao, X. Liu and Q. Zhang, *Talanta*, 2012, **93**, 350–357.
32 X. Cai, M. Lin, S. Tan, W. Mai, Y. Zhang, Z. Liang, Z. Lin and X. Zhang, *Carbon*, 2012, **50**, 3407–3415.
33 X. Yang, Y. Tu, L. Li, S. Shang and X. Tao, *ACS Appl. Mater. Interfaces*, 2010, **2**(6), 1707–1713.
34 H. Im and J. Kim, *Carbon*, 2012, **50**, 5429–5440.
35 J. Qin, X. Zhang, Y. Xue, N. Kittiwattanothai, P. Kongsittikul, N. Rodthongkum, S. Limpanart, M. Ma and L. Riping, *Appl. Surf. Sci.*, 2014, **321**, 226–232.
36 A. Fonseca de Faria, D. S. T. Martinez, M. MeiraStela Maris, A. C. Mazarin de Moraes, A. Brandelli, A. G. S. Filho and O. L. Alves, *Colloids Surf., B*, 2014, **113**, 115–124.
37 D. Han, L. Yan, W. Chen and W. Li, *Carbohydr. Polym.*, 2011, **83**, 653–658.
38 S. Baradaran, E. Moghaddam, W. J. Basirun, M. Mehrali, M. Sookhakian, M. Hamdi, M. R. Nakhaei Moghaddam and Y. Alias, *Carbon*, 2014, **69**, 32–45.
39 M. B. Patel, U. Harikrishnan, N. N. Valand, N. R. Modi and S. K. Menon, *Arch. Pharm. Chem. Life Sci.*, 2013, **346**(3), 210–220.
40 J. Gupta, P. Bhargava and D. Bahadur, *J. Mater. Chem. B*, 2015, **3**, 1968–1978.
41 L. Huang, D. Q. Li, Y. J. Lin, M. Wei, D. G. Evans and X. Duan, *J. Inorg. Biochem.*, 2005, **99**, 986–993.
42 S. Makhluf, R. Dror, Y. Nitzan, Y. Abramovich, R. Jelinek and A. Gedanken, *Adv. Funct. Mater.*, 2005, **15**, 1708–1715.

